www.nature.com/modpathol

ARTICLE

Lymphocyte-activation gene 3 in non-small-cell lung carcinomas: correlations with clinicopathologic features and prognostic significance

Daniel J. Shepherd[1,2], Elisabeth S. Tabb[1,2], Keiko Kunitoki[3], M. Lisa Zhang[1,2], Marina Kem[1], Jaimie Barth[1], David A. Qualls[4,6], Meghan J. Mooradian[4,5], Justin F. Gainor[4,5], Mari Mino-Kenudson[1,2,5,7]✉ and Yin P. Hung[1,2,5,7]

Lymphocyte-activation gene 3 (LAG-3) modulates the tumor microenvironment through immunosuppressive effects. Its associations with clinicopathologic parameters and prognostic significance in non-small-cell lung carcinomas remain unclear. We examined LAG-3 expression in 368 resected non-small-cell lung carcinomas (including 218 adenocarcinomas and 150 squamous-cell carcinomas) using tissue microarrays, with normalization to $CD8^+$ T-cell count (LAG-3/CD8 index), and correlated LAG-3, CD8, and LAG-3/CD8 index with clinicopathologic features, molecular status, and survival. LAG-3 expression in the immune cells (ranged 0.35–540.1 cells/mm^2) was identified in 92% of non-small-cell lung carcinomas. In adenocarcinomas and squamous-cell carcinomas, LAG-3 expression correlated with $CD8^+$ T-cell count and PD-L1 expression. In adenocarcinomas, high LAG-3 expression (defined as >median) was additionally associated with smoking history, high T stage, aggressive pathologic features (solid-predominant histologic pattern, lymphovascular invasion, and nodal metastasis), and lack of *EGFR* mutation. In the entire resected tumor cohort and in adenocarcinomas, high LAG-3 and LAG-3/CD8 index were each associated with worse overall survival. In squamous-cell carcinomas, high CD8 was associated with better overall survival. In an exploratory analysis of pretreatment samples from advanced non-small-cell lung carcinoma patients treated with pembrolizumab, high CD8 was predictive of improved overall and progression-free survival, while high LAG-3, but not high LAG-3/CD8 index, was associated with improved progression-free survival. In conclusion, the clinicopathologic correlations and prognostic impact of LAG-3 in non-small-cell lung carcinoma are histotype-dependent, highlighting differences in the immune microenvironment between adenocarcinomas and squamous-cell carcinomas. The predictive impact of LAG-3 warrants further investigation.

Modern Pathology (2022) 35:615–624; https://doi.org/10.1038/s41379-021-00974-9

INTRODUCTION

Therapies targeting immune checkpoints such as programmed cell death protein 1 and ligand (PD-1/PD-L1) and cytotoxic T-lymphocyte-associated protein-4 (CTLA-4) are standard therapies for advanced non-small-cell lung carcinomas, but only a fraction of patients benefit from these agents.[1–5] While efforts to identify biomarkers that can predict treatment response have led to approval and widespread clinical adoption of PD-L1 immunohistochemical assays as companion diagnostics for anti-PD-1/PD-L1 therapy,[6] PD-L1 immunohistochemistry remains an imperfect predictor of treatment response, underscoring the need for additional biomarkers of immune responsiveness in non-small-cell lung carcinomas.[7]

Lymphocyte-activation gene 3 (LAG-3), or CD223, is a transmembrane receptor expressed by several immune cell types in the tumor microenvironment, including $CD4^+$, $CD8^+$, and regulatory T cells (Treg).[8,9] Known LAG-3-activating ligands include major histocompatibility complex (MHC) class II, galectin-3, and fibrinogen-like protein 1.[10–12] Analogous to PD-1, LAG-3 activation transmits inhibitory signals that suppress antitumor immunity.[8] Chronic T-cell stimulation, such as in certain viral infections or cancer, leads to upregulation of cell surface LAG-3 and eventual T cell exhaustion, while LAG-3 dysregulation can exacerbate autoimmunity.[8,13] LAG-3 expression by tumor-infiltrating and tumor-associated lymphocytes has been reported in several tumor types, including non-small-cell lung carcinoma.[14–23] In preclinical models, LAG-3 inhibition enhances antitumor immunity and synergizes with PD-1 blockade.[8] In 90 non-small-cell lung carcinoma patients, LAG-3 expression has been reported to be associated with shorter progression-free survival in those treated with PD-1 axis blockers as various lines of therapy, suggesting that increased LAG-3 expression may antagonize the efficacy of anti-PD-1 treatment.[20] Given the immunosuppressive role of LAG-3, clinical trials targeting LAG-3 in solid tumors have been designed with some completed.[8,24] The soluble LAG-3-Fc fusion protein IMP321 (eftilagimod alpha), thought to enhance

[1]Department of Pathology, Massachusetts General Hospital, Boston, USA. [2]Department of Pathology, Harvard Medical School, Boston, MA, USA. [3]Harvard T.H. Chan School of Public Health, Boston, MA, USA. [4]Department of Medicine, Massachusetts General Hospital and Harvard Medical School, Boston, MA, USA. [5]Massachusetts General Hospital Cancer Center, Boston, MA, USA. [6]Present address: Department of Medicine, Memorial Sloan Kettering Cancer Center, New York, NY, USA. [7]These authors contributed equally: Mari Mino-Kenudson, Yin P. Hung. ✉email: mminokenudson@partners.org

Received: 29 March 2021 Accepted: 11 November 2021
Published online: 8 December 2021

antigen-presenting cell activity and cross presentation to $CD8^+$ T cells and suppress Treg activity, has demonstrated limited efficacy in renal cell carcinoma, metastatic breast cancer, and melanoma. Trials using the LAG-3-specific neutralizing antibody relatlimab are underway, with LAG-3 expression in ≥1% of tumor-infiltrating lymphocytes found to correlate with a higher objective response rate in melanoma.[8] While clinical trials of LAG-3-targeting therapies in non-small-cell lung carcinomas are ongoing (NCT03625323, NCT01968109, NCT02750514, NCT02460224, and NCT03538028), the association of LAG-3 expression with clinicopathologic parameters and its prognostic significance in non-small-cell lung carcinoma remain unclear.

In this study, we examined LAG-3 expression in a cohort of non-small-cell lung carcinomas, aiming to characterize its clinicopathologic and prognostic significance. In an exploratory analysis, we evaluated pretreatment samples from advanced lung-carcinoma patients treated with immunotherapy to examine the predictive impact of LAG-3 expression.

MATERIALS AND METHODS

Study population and sample selection

This study was approved by the Massachusetts General Hospital Institutional Review Board. The Massachusetts General Hospital surgical pathology database was queried for primary lung adenocarcinomas resected between January 2010 and December 2012 and squamous-cell carcinomas resected between February 2005 and June 2014. After exclusion of post-neoadjuvant therapy resections, those with incomplete resection and/or multiple synchronous tumors, adenocarcinomas without molecular annotation, and those without available tumor tissue for TMA construction, a total of 452 primary non-small-cell lung-carcinomas (consisting of 261 adenocarcinomas and 191 squamous cell carcinomas) were included in the study cohort. Furthermore, a separate cohort of 38 advanced non-small-cell lung carcinoma patients with available pretreatment samples (biopsy or resection) procured between June 2015 and September 2019 and PD-L1 tumor-proportion score ≥50,[25] who were subsequently treated with the anti-PD-1 monoclonal antibody pembrolizumab as the first-line therapy, was examined using whole tissue sections in an exploratory analysis.

Clinical information, demographics, and follow-up outcome data (as updated on November 1st, 2020) were obtained from medical records. Smoking history was defined as tobacco use of at least 10 pack-years.[26] Progression-free and recurrence-free survival were defined as the time from pathologic diagnosis to clinical and/or radiologic progression or death; patients without disease progression/recurrence were censored on the date of the last follow-up. Overall survival was defined as the time between pathologic diagnosis and death from any cause. Histologic review including evaluation of tumor size (including total size and invasive size in adenocarcinomas), stage (pT and pN), predominant histologic pattern (in adenocarcinomas), histologic differentiation, and presence or absence of lymphatic, vascular, or pleural invasion was performed by pulmonary pathologists as described.[27] Histologic patterns were classified in accordance with International Association for the Study of Lung Cancer/American Thoracic Society/European Respiratory Society joint consensus.[28] Complex glandular pattern that has recently been described as high-grade pattern was included in the histologic pattern assessment.[29] Tumor stage was determined in accordance with the American Joint Committee on Cancer (AJCC) Cancer Staging Manual 8th edition.[30] Molecular analysis was previously performed in the adenocarcinomas to detect commonly mutated genes (including *EGFR*, *KRAS*, *BRAF*, *ERBB2*, and *TP53*) using a polymerase-chain reaction-based assay (SNaPshot platform; Applied Biosystems, Waltham, MA, USA), as described.[27,31]

Immunohistochemistry and quantification

Tissue microarrays were constructed using two 2-millimeter cores (including the center and the infiltrative front) from each of the 452 non-small-cell lung carcinomas as described;[27] tonsil, placenta, and lung were included as controls. Immunohistochemistry was performed on 5-micron-thick formalin-fixed paraffin-embedded sections from tissue microarray blocks using an automated stainer (Bond Rx; Leica Microsystems, Bannockburn, IL) and the following antibodies (clone, dilution, vendor): LAG-3 (D2G4O, 1:200, Cell Signaling Technology, Danvers, MA); CD8 (4B11, ready-to-use, Leica Biosystems, Buffalo Grove, IL); and PD-L1 (E1L3N, 1:200, Cell Signaling Technology). Immunoreactivity of PD-L1 was evaluated using an H-score system (range 0–300), which integrated the percentage of cells with membranous PD-L1 staining (range 0–100%) and the staining intensity (range 0–3). Selected data on PD-L1 for the adenocarcinoma tissue microarray cohort were published.[27,32] H-scores of the squamous cell carcinoma cohort were determined by two pathologists (DJS and MM-K) blind to clinical data.

Tumor-associated lymphocytes encompass both intratumoral (i.e., intraepithelial) and stroma-associated lymphocytes. For assessment of LAG-3 expression, a pathologist (DJS) blind to clinical information manually counted tumor-associated lymphocytes expressing LAG-3 in three 400× high-power fields (0.24 mm^2 per field) and calculated $LAG\text{-}3^+$ cell density (cells per mm^2). As manual counting of $CD8^+$ tumor-associated lymphocytes was not practically feasible given their large numbers in many cases, $CD8^+$ tumor-associated lymphocytes were quantified using a semiautomated counting method: CD8 immunohistochemical stains were scanned using the Philips IntelliSite Ultra Fast Scanner 1.8.1.3 (Philips, Eindhoven, The Netherlands). Digitized images were exported at 100× magnification using ImageJ (National Institutes of Health),[33] and the total number of signal-positive pixels in the regions of interests (ROI) encompassing the tumor was quantified. ROI was defined as the entire area of the tumor represented in the disc (each measuring 2 mm in diameter), including associated stroma. $CD8^+$ cell count was determined by dividing the total number of signal-positive pixels within the ROI by the average number of signal-positive pixels per $CD8^+$ T cell, an empiric factor we previously determined. $CD8^+$ T-cell density (cells per mm^2) was calculated by dividing the $CD8^+$ cell count by the ROI area. As validation for this method, our calculated $CD8^+$ T-cell densities were concordant with manually determined semiquantitative scores (range 0–3) on the number of $CD8^+$ tumor-infiltrating lymphocytes.[34] To evaluate for LAG-3-specific effects and account for $CD8^+$ T-cell abundance, we determined for each tumor a LAG-3/CD8 index by normalizing the $LAG\text{-}3^+$ cell density to the estimated $CD8^+$ cell density and multiplying by 100. To assess for intratumoral compartmental differences, intraepithelial and stromal $LAG\text{-}3^+$ and $CD8^+$ cell densities were determined by visually estimating the proportion of LAG-3 and CD8 in each of the two compartments, dividing by the estimated proportional area of each compartment, and multiplying by the overall marker density. The same evaluation methods for LAG-3 and CD8 were applied to both tissue microarray samples from the resected cohort and whole-slide sections from pretreatment samples of the pembrolizumab-treated cohort.

Statistical analysis

Medians of LAG-3, CD8, and LAG-3/CD8 index were calculated separately for each cohort (adenocarcinomas, squamous-cell carcinomas, entire resected non-small-cell lung carcinoma cohort, and immunotherapy-treated cohort). Low and high expression were defined as below/equal to and above the median for each cohort, respectively. Comparisons were performed using Wilcoxon rank-sum tests between LAG-3, CD8, or LAG-3/CD8 index as continuous variables and the following binary variables: smoking status, lymphovascular invasion (LVI), pleural invasion, lymph node metastasis, pT status, and predominant histologic pattern (in adenocarcinomas) or differentiation (in squamous-cell carcinomas). Comparisons in proportions and among continuous variables were performed using Fisher exact tests and Spearman correlation analysis, respectively. Overall survival, recurrence-free survival, and progression-free survival were estimated by the Kaplan–Meier method, with differences analyzed by log-rank tests. Multivariable analyses with the Cox proportional hazard regression model were used to calculate hazard ratios and 95% confidence intervals for candidate prognostic factors. Statistical analysis was performed using GraphPad Prism version 8 (GraphPad Software, San Diego, CA) and R version 3.6.1 (www.R-project.org; R core team, Vienna, Austria,[35]) using the R packages "survival" version 2.38 and "survminer" version 0.4.6. Statistical significance was set at $p < 0.05$.

RESULTS

Correlation of $LAG\text{-}3^+$ and $CD8^+$ cell densities with clinicopathologic and molecular parameters in adenocarcinomas

In the adenocarcinoma cohort, after excluding cases due to insufficient material on tissue microarrays or poor staining quality,

LAG-3 immunohistochemistry was evaluable in 218 patients (63% female, median age 70 years), with the following distribution of predominant histologic patterns: 20% lepidic, 21% acinar, 15% complex glandular/high-grade acinar (HGA), 17% papillary, 4% micropapillary, 17% solid, and 6% invasive mucinous. The cohort composition is detailed in Supplemental Table 1. At least some (>0 cells/mm^2) expression of LAG-3 (Fig. 1A) was present in 195 (89%) samples, with a median density of 7.0 cells/mm^2 (range 0.0–540.1 cells/mm^2) across all adenocarcinomas. By univariate analysis, high LAG-3 expression was significantly associated with ≥10 pack-year smoking history ($p = 0.001$), tumors with solid-predominant histologic pattern ($p < 0.0001$), presence of LVI ($p < 0.001$), lymph-node metastasis ($p = 0.011$), and non-T1 tumor stages ($p = 0.020$) (Fig. 1B, Supplemental Fig. 1). In adenocarcinomas, the median density of CD8$^+$ tumor-associated lymphocytes was 505.9 cells/mm^2 (range 27.8–4164.2 cells/mm^2) (Fig. 1A). High CD8 was significantly associated with solid-predominant histologic pattern ($p < 0.0001$) and the presence of LVI ($p = 0.039$) (Fig. 1B). By univariate analysis, LAG-3 correlated positively with CD8 ($r_s = 0.535$, $p < 0.0001$) (Supplemental Fig. 2A).

As LAG-3 is expressed by a subset of CD8$^+$ tumor-associated T-cells in non-small-cell lung carcinomas,[20,23] and LAG-3 expression appears to be correlated with CD8 expression, we assessed for LAG-3$^+$ specific effects by calculating a "LAG-3/CD8 index" after normalizing the LAG-3$^+$ cell density to the corresponding CD8$^+$ cell density. Among the 213 adenocarcinomas with both LAG-3 and CD8 data available, the median LAG-3/CD8 index was 1.7 (range 0-43.0). High LAG-3/CD8 index was significantly associated with ≥10 pack-year smoking history ($p = 0.001$), non-T1 tumor stages ($p = 0.004$), solid-predominant histologic pattern ($p < 0.0001$), presence of LVI ($p = 0.005$), and lymph node metastasis ($p = 0.004$) (Fig. 1B). Tumoral PD-L1 expression as assessed by H-score weakly correlated with LAG-3 expression ($r_s = 0.190$, $p = 0.005$), CD8 expression ($r_s = 0.138$, $p = 0.042$), and LAG-3/CD8 index ($r_s = 0.190$, $p = 0.006$) (Fig. 1B, Supplemental Fig. 3A).

The overall frequency of molecular alterations in this adenocarcinoma cohort was as follows: 40.8% *KRAS*-mutated, 21.6% *EGFR*-mutated, 1.4% *ALK*-rearranged, 5.5% others, and 30.7% with none identified (Supplemental Fig. 4A). Both the median LAG-3$^+$ cell density and LAG-3/CD8 index were significantly lower in *EGFR*-mutated tumors compared with *EGFR* wild-type tumors ($p = 0.0019$ and $p = 0.0002$, respectively). No differences in CD8$^+$ cell density according to molecular status were detected (Fig. 1B, Supplemental Fig. 4B–C).

Multivariate logistic-regression analysis showed that high LAG-3 was independently associated with ≥10 pack-year smoking history (OR 3.32, CI 1.38–8.67, $p = 0.010$) and a solid-predominant histologic pattern (OR 2.76, CI 1.10–7.49, $p = 0.037$), while high CD8 was independently associated with a solid-predominant histologic pattern (OR 4.58, CI 1.82–12.71, $p = 0.002$). High LAG-3/CD8 index was independently associated with lack of EGFR mutation (OR 0.38, CI 0.15–0.91, $p = 0.034$) (Fig. 1C).

Correlation of LAG-3$^+$ and CD8$^+$ cell densities with clinicopathologic parameters in squamous-cell carcinomas

The squamous cell carcinoma cohort with evaluable LAG-3 included 150 patients (43% female, median age 70 years), with 70% well-/moderately-differentiated and 30% poorly-differentiated tumors. Compared with the adenocarcinoma cohort, the squamous-cell carcinoma cohort contained more males ($p < 0.001$) and patients at advanced stages (II–IV) ($p < 0.0001$). At least some (>0 cells/mm^2) expression of LAG-3 (Fig. 2A) was present in 145 (97%) samples, with a median density of 27.5 cells/mm^2 (range 0–326 cells/mm^2) across all squamous cell carcinomas. The median density of CD8$^+$ tumor-associated lymphocytes was 565.6 cells/mm^2 (range 16–2983 cells/mm^2). By univariate analysis, LAG-3 correlated positively with CD8 count ($r_s = 0.641$, $p < 0.0001$) (Supplemental Fig. 2B). Among the 150 squamous cell carcinomas with both LAG-3 and CD8 data available, the median LAG-3/CD8 index was 5.45 (range 0.0–102.6). No significant associations of LAG-3, CD8, or LAG-3/CD8 index with age, sex, smoking history, lymph node metastasis, pT status, degree of differentiation, pleural invasion, or LVI were noted (Fig. 2B). Tumoral PD-L1 H-score correlated with LAG-3 ($r_s = 0.387$, $p < 0.0001$), CD8 ($r_s = 0.307$, $p < 0.0001$), and LAG-3/CD8 index ($r_s = 0.300$, $p = 0.002$) (Fig. 2B, Supplemental Fig. 3B).

Multivariate logistic-regression analysis showed that high LAG-3 was independently associated with the absence of pleural invasion (OR 0.21, CI 0.06–0.62, $p = 0.007$) and the absence of LVI (OR 0.32, CI 0.11–0.87, $p = 0.030$). A high LAG-3/CD8 index was independently associated with non-T1 tumor stages (OR 2.90, CI 1.07–8.24, $p = 0.040$). High LAG-3, high CD8, and high LAG-3/CD8 index were each independently associated with high PD-L1 (OR 4.60, CI 1.71–13.65, $p = 0.004$; OR 3.84, CI 1.64–9.58, $p = 0.003$; OR 2.87, CI 1.07–8.24, $p = 0.026$, respectively) (Fig. 2C).

Overall non-small-cell lung-carcinoma cohort

In the resected non-small-cell lung carcinoma cohort of 452 patients, after excluding cases due to insufficient material or poor staining quality, a total of 368 and 405 samples were analyzed for LAG-3 and CD8 expression, respectively. Of the entire resected cohort, stage-I patients comprised 69%, and 83% were smokers of ≥10 pack-years (Supplemental Table 1). Multivariate logistic regression analysis performed on the entire cohort showed that high LAG-3 was independently associated with ≥10 pack-year smoking history (OR 2.09, CI 1.06–4.29, $p = 0.038$) and squamous histology (OR 4.17, CI 2.40–7.40, $p < 0.0001$) (Supplemental Fig. 5). High CD8 was independently associated with ≥10 pack-year smoking history (OR 2.02, CI 1.07–3.90, $p = 0.032$) and PD-L1 H-score ≥5 (OR 2.28, CI 1.39-3.77, p = 0.001). High LAG-3/CD8 index was independently associated with ≥10 pack-year smoking history (OR 2.91, CI 1.39–6.43, $p = 0.006$), lymph node metastasis (OR 2.38, CI 1.10–5.32, $p = 0.03$), non-T1 tumor stages (OR 2.38, CI 1.21–4.75, $p = 0.012$), and squamous histology (OR 7.16, CI 3.94–13.47, $p < 0.0001$) (Supplemental Fig. 5).

Prognostic significance of LAG-3 in non-small-cell lung carcinomas

By univariate analysis, high LAG-3 and high LAG-3/CD8 index were each associated with worse overall survival ($p = 0.036$ and $p < 0.0001$, respectively) in the entire non-small-cell lung carcinoma cohort (Fig. 3A, D), while no association with CD8 was identified (Fig. 3B). Notably, in adenocarcinomas, high LAG-3 and high LAG-3/CD8 index remained associated with worse overall survival ($p = 0.006$ and $p = 0.008$, respectively) (Fig. 3F, I), while CD8 expression was not associated with overall survival (Fig. 3G). No associations between LAG-3, CD8, or LAG-3/CD8 index and recurrence-free survival were seen in the entire non-small-cell lung carcinoma cohort or in adenocarcinomas (Supplemental Fig. 6A–J). In contrast, in squamous cell carcinomas, no associations between LAG-3 or LAG-3/CD8 index with overall survival were noted (Fig. 3K, N). Instead, high CD8 was significantly associated with better overall survival ($p = 0.002$) (Fig. 3L) and recurrence-free survival ($p = 0.017$) (Supplemental Fig. 6L). Our findings on the worse survival in adenocarcinomas with high LAG-3 or high LAG-3/CD8 index and on the better survival in squamous cell carcinomas with high CD8 appeared robust and remained unchanged, regardless of the median cutoffs of the tumor types chosen (Supplemental Fig. 7).

Multivariate Cox proportional hazard analyses were performed using either LAG-3 and CD8 or LAG-3/CD8 index as covariates with various clinicopathologic parameters. In the entire non-small-cell lung-carcinoma cohort, low CD8 (HR 0.61, CI 0.40–0.94, $p = 0.024$), high LAG-3/CD8 index (HR 1.61, CI 1.05–2.45, $p = 0.028$), ≥10 pack-year smoking history (HR 2.23, CI 1.13–4.40, $p = 0.021$), squamous histology (HR 1.65, CI 1.09–2.48, $p = 0.017$), and stages II–IV (HR

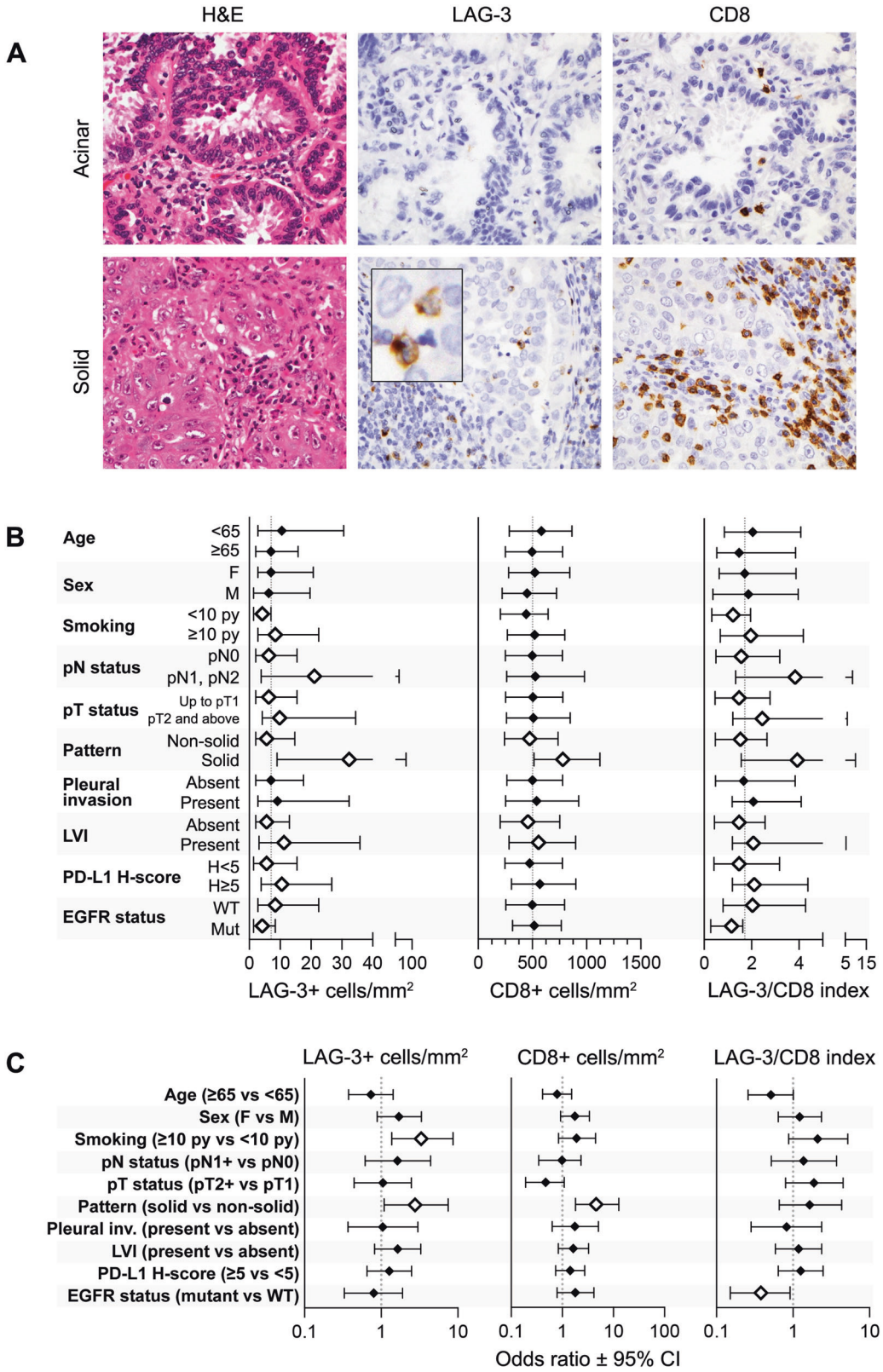

Fig. 1 Associations of LAG-3 expression with clinicopathologic and molecular features in primary lung adenocarcinomas. **A** Representative images of LAG-3 and CD8 immunohistochemical staining in acinar- (top row) and solid- (bottom row) pattern adenocarcinomas. H&E: hematoxylin and eosin. **B** LAG-3 (left), CD8 (middle), and LAG-3/CD8 index (right) stratified by clinicopathologic and molecular features. Diamonds and bars represent medians and interquartile ranges, respectively. Vertical dotted lines indicate medians of the cohort. Open diamonds indicate $p < 0.05$ (Wilcoxon rank-sum tests). **C** Multivariate logistic regression analysis. Diamonds and bars represent odds ratios and 95% confidence intervals, respectively. Open diamonds indicate $p < 0.05$ (logistic-regression analysis). pN1+ encompasses pN1 and pN2; pT2+ encompasses pT2, pT3, and pT4. Pleural inv. pleural invasion, LVI lymphovascular invasion, WT wild type, mut: mutated.

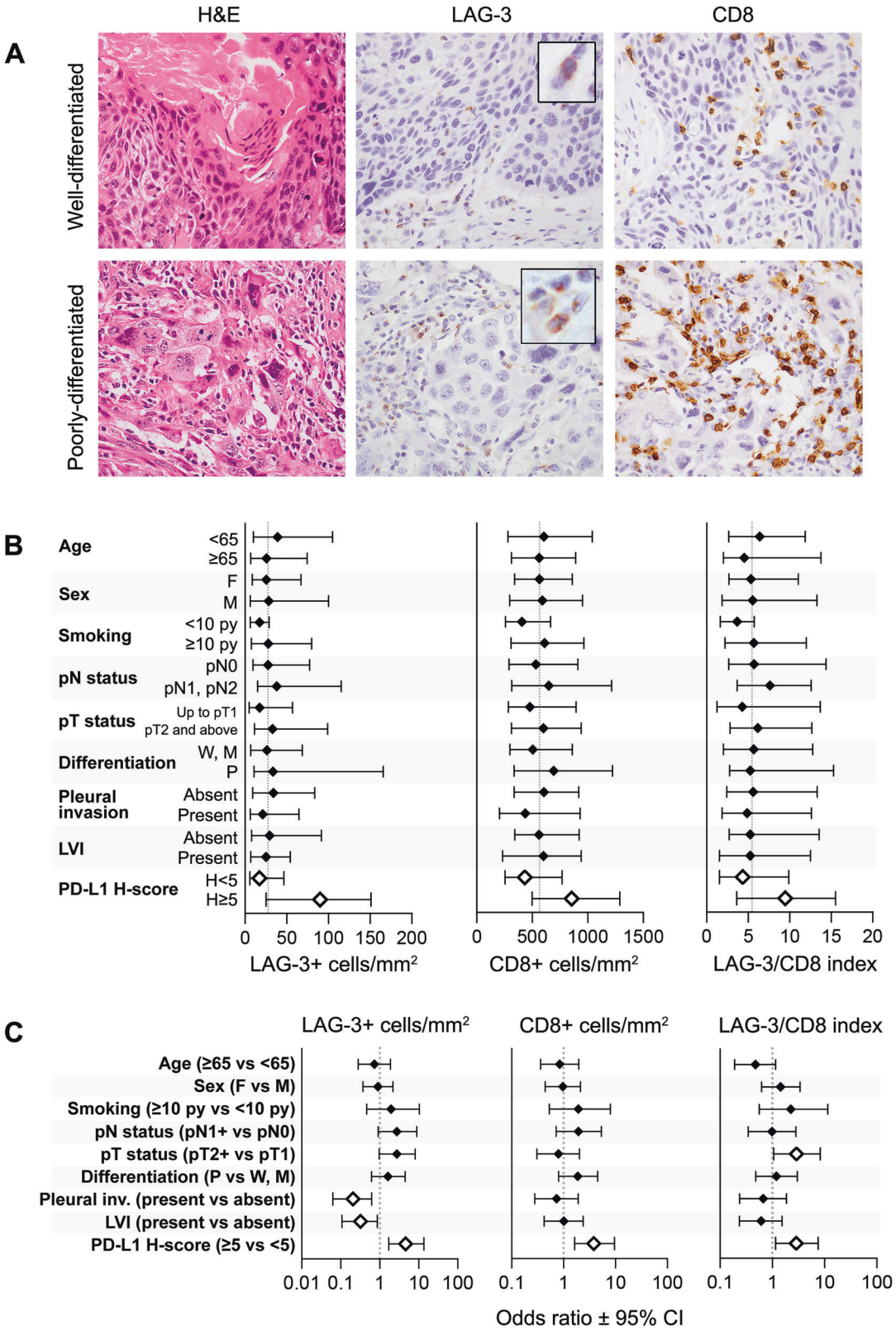

Fig. 2 Associations of LAG-3 expression with clinicopathologic and molecular features in primary lung squamous-cell carcinomas. **A** Representative images of LAG-3 and CD8 immunohistochemical staining in well-differentiated (top row) and poorly-differentiated (bottom row) squamous cell carcinomas. H&E: hematoxylin and eosin. **B** LAG-3 (left), CD8 (middle), and LAG-3/CD8 index (right) stratified by clinicopathologic and molecular features. Diamonds and bars represent medians and interquartile ranges, respectively. Vertical dotted lines indicate medians of the cohort. Open diamonds indicate $p < 0.05$ (Wilcoxon rank-sum tests). **C** Multivariate logistic regression analysis. Diamonds and bars represent odds ratios and 95% confidence intervals, respectively. Open diamonds indicate $p < 0.05$ (logistic regression analysis). W well-differentiated, M moderately differentiated, P poorly-differentiated, Pleural inv. pleural invasion, LVI lymphovascular invasion.

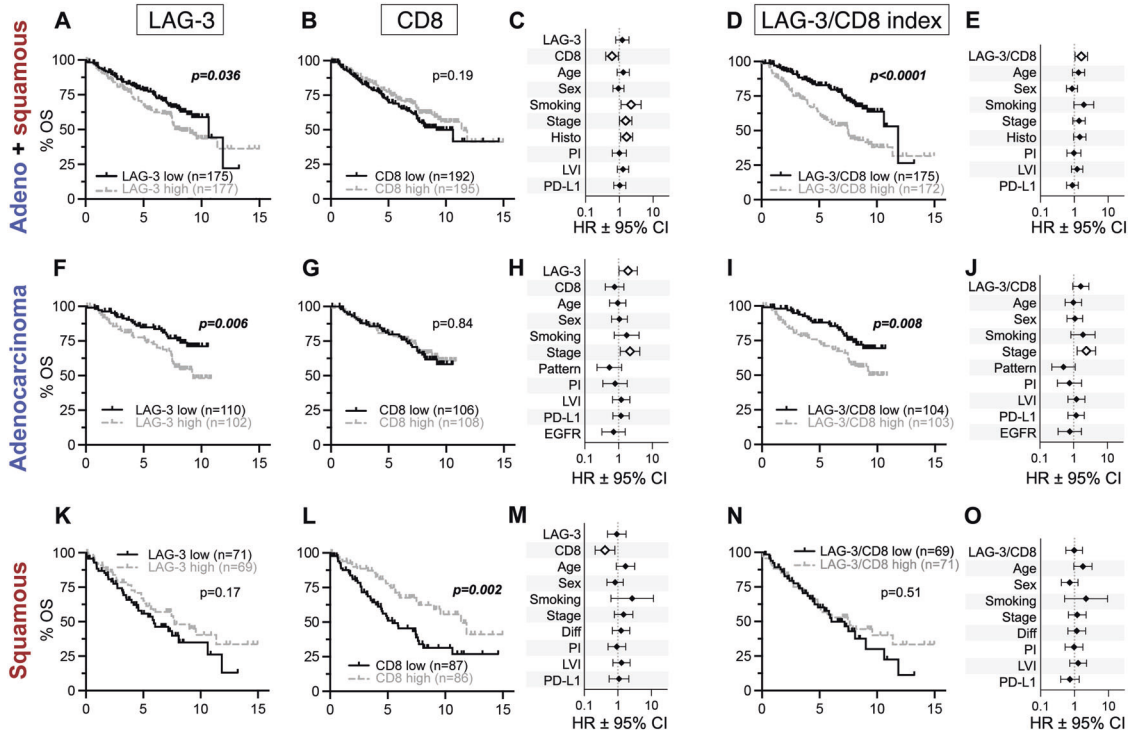

Fig. 3 Overall survival and multivariate analysis in patients with resected non-small-cell lung carcinomas stratified by LAG-3, CD8, and LAG-3/CD8 index. A–E Overall survival (OS) in the combined adenocarcinoma and squamous-cell carcinoma cohort stratified by LAG-3 (**A**), CD8 (**B**), and LAG-3/CD8 index (**D**). Forest plots of hazard ratios (HR), including LAG-3 and CD8 separately (**C**) and LAG-3/CD8 index (**E**) as covariates. **F–J** OS in adenocarcinomas stratified by LAG-3 (**F**), CD8 (**G**), and LAG-3/CD8 ratio (**I**). Forest plots of HR, including LAG-3 and CD8 separately (**H**) and LAG-3/CD8 index (**J**) as covariates. **K–O** OS in squamous-cell carcinomas stratified by LAG-3 (**K**), CD8 (**L**), and LAG-3/CD8 index (**N**). Forest plots of HR, including LAG-3 and CD8 separately (**M**) and LAG-3/CD8 index (**O**) as covariates. "Low" and "high" refer to ≤ and >median, respectively. Sample sizes represent the number at risk at time 0. Open diamonds indicate $p < 0.05$ (Cox proportional hazards).

1.54, CI 1.01–2.36, $p = 0.046$) were independently associated with worse overall survival (Fig. 3C, E). When separated by histotypes, high LAG-3 (HR 1.92, CI 1.03–3.58, $p = 0.040$) and stages II–IV (HR 2.18, CI 1.12-4.24, $p = 0.021$) were independently associated with worse overall survival in adenocarcinomas (Fig. 3H, J). Low CD8 (HR 0.41, CI 0.21–0.82, $p = 0.011$), but not LAG-3/CD8 index, was independently associated with worse overall survival in squamous cell carcinomas (Fig. 3M, O).

By multivariate analysis, the presence of lymphovascular invasion was independently associated with worse recurrence-free survival in the entire non-small-cell lung carcinoma cohort and in adenocarcinomas (HR 2.25, CI 1.30–3.88, $p = 0.003$; HR 4.55, CI 2.01–10.29, $p < 0.001$, respectively). Neither LAG-3 nor CD8 showed significant associations (Supplemental Fig. 6). No significant associations with recurrence-free survival were identified in the squamous cell carcinoma cohort (Supplemental Fig. 6).

Prognostic significance of stromal versus intraepithelial LAG-3$^+$ and CD8$^+$ cells in non-small-cell lung carcinomas

We next evaluated and analyzed separately the stroma-associated (stromal) and the tumor-infiltrating (intraepithelial) compartments of the LAG-3$^+$ and CD8$^+$ tumor-associated lymphocytes in non-small-cell lung carcinomas. Both stromal LAG-3$^+$ and CD8$^+$ cell densities were higher than their corresponding intraepithelial densities in adenocarcinomas and squamous cell carcinomas (Supplemental Fig. 8A–F). Both stromal and intraepithelial LAG-3$^+$ cell densities and LAG-3/CD8 indices in squamous cell carcinomas were higher than those in adenocarcinomas (Supplemental Fig. 8C, G–I).

In the entire resected non-small-cell carcinoma cohort and in adenocarcinomas alone, high intraepithelial and stromal LAG-3 were each associated with worse overall survival (Supplemental Fig. 9A B, G H). High intraepithelial and stromal LAG-3/CD8 indices were each associated with worse overall survival in the entire resected tumor cohort (Supplemental Fig. 9E–F). In adenocarcinomas, high intraepithelial LAG-3/CD8 index, but not stromal LAG-3/CD8 index, was associated with worse overall survival (Supplemental Fig. 9K–L). In contrast, in squamous cell carcinomas, better overall survival was seen in tumors with high stromal CD8, but not in tumors with intraepithelial CD8 (Supplemental Fig. 9O–P). Unlike adenocarcinomas, no associations between intraepithelial or stromal LAG-3/CD8 index with overall survival were noted in squamous-cell carcinomas (Supplemental Fig. 9Q–R).

Evaluation of LAG-3 in pretreatment samples from pembrolizumab-treated non-small-cell lung-carcinoma patients

To explore the predictive impact of LAG-3 expression, we analyzed pretreatment samples from 38 patients with advanced non-small-cell lung carcinomas with PD-L1 tumor-proportion score of ≥50% and treated with first-line pembrolizumab. The cohort composition is detailed in Supplemental Table 2. Due to limited tissue available, both LAG-3 and CD8 were evaluable in 32 patient cases, which included 24 adenocarcinomas (including 4 primaries and 20 metastases), four squamous cell carcinomas (including two primaries and two metastases), 1 non-small-cell lung carcinoma, not otherwise specified (metastasis), and three pleomorphic carcinomas (including two primaries and one metastasis) (Fig. 4A, Supplemental Fig. 10). The median number of LAG-3$^+$ cells and the median LAG-3/CD8 index were 39.0 cells/mm^2 (range 0.0–1039.4 cells/mm^2) and 9.0, respectively, which were higher than those in the resected tumor cohort ($p = 0.005$, $p < 0.0001$, respectively) (Fig. 4B), while no significant differences in the number of CD8$^+$ cells were identified between the advanced non-small-cell lung

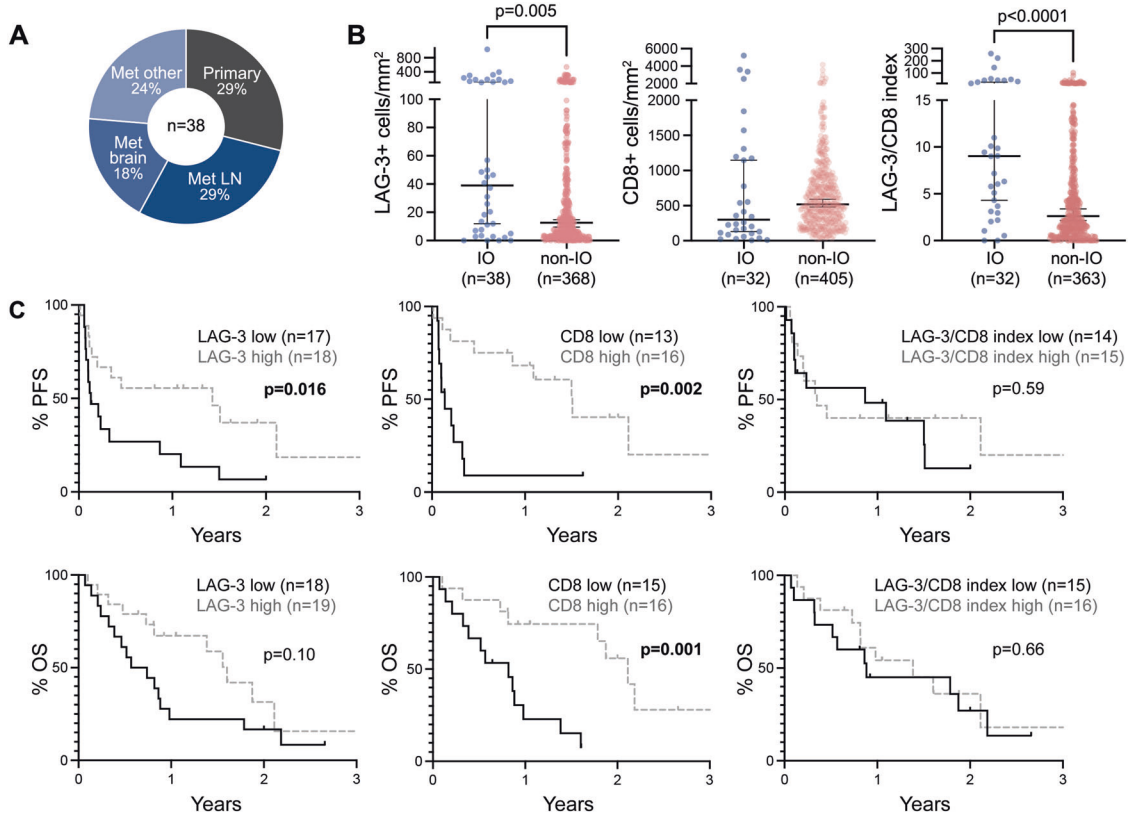

Fig. 4 LAG-3 expression in pretreatment samples from pembrolizumab-treated advanced non-small-cell lung carcinoma patients. **A** Distribution of primary and metastatic pretreatment samples in the pembrolizumab-treated patient cohort ($n = 38$ with evaluable LAG-3). Met metastasis, LN lymph node. **B** LAG-3 (left), CD8 (middle), and LAG-3/CD8 index (right) in the pembrolizumab-treated (IO) and non-IO cohorts. Bars represent medians and 95% confidence intervals. **C** Progression-free (top) and overall (bottom) survival in the IO cohort stratified by LAG-3, CD8, and LAG-3/CD8. "Low" and "high" refer to ≤ and >median, respectively. Sample sizes represent the number at risk at time 0.

carcinoma cohort and the resected tumor cohort. Similar to what was observed in the resected tumor cohort, expression of LAG-3 and CD8 correlated with PD-L1 tumor proportion score in these pretreatment biopsies (Supplemental Fig. 11). In this first-line pembrolizumab cohort, high LAG-3 was associated with better progression-free survival ($p = 0.016$) (Fig. 4C). When analyzed separately by compartments, high stromal LAG-3, but not intraepithelial LAG-3, was associated with better progression-free survival ($p = 0.013$) (Supplemental Fig. 12). Nonetheless, there were no significant associations between LAG-3 and overall survival, as well as between LAG-3/CD8 index and progression-free survival or overall survival (Fig. 4C), including evaluated separately in the intraepithelial versus stromal compartments (Supplemental Fig. 12). On the other hand, high CD8 overall, high stromal CD8, and high intraepithelial CD8 in the pretreatment samples were each significantly associated with better progression-free survival and overall survival in the pembrolizumab-treated cohort (Fig. 4C, Supplemental Fig. 12).

DISCUSSION

In this study, we correlated the density of LAG-3$^+$ tumor-associated lymphocytes with clinicopathologic factors, molecular features, and survival in 368 non-small-cell lung carcinomas. To assess for LAG-3$^+$-specific effects and account for CD8$^+$ T-cell abundance, we normalized LAG-3$^+$ cell density to CD8$^+$ cell density. In the entire resected non-small-cell lung carcinoma cohort, high LAG-3 expression was associated with worse overall survival and selected aggressive features, including higher pT stages and lymph node metastasis (Supplemental Fig. 5). When analyzed by histotypes, the associations between LAG-3 and survival were largely accounted for by adenocarcinomas, but not squamous cell carcinomas (Fig. 3). Despite the known immunosuppressive role of LAG-3 in the tumor immune microenvironment, our findings on the histotype-dependent correlations and prognostic significance of LAG-3 highlight the differences in tumor microenvironment between lung adenocarcinomas and squamous cell carcinomas.[36]

In addition, we identified the majority of LAG-3$^+$ and CD8$^+$ tumor-associated lymphocytes to be within the stroma rather than the intraepithelial compartment. Both stromal and intraepithelial LAG-3$^+$ cell counts were higher in squamous cell carcinomas than in adenocarcinomas (Supplemental Fig. 8). In the entire resected tumor cohort and in adenocarcinomas alone, we identified no consistent differences between the intratumoral compartmentalization of LAG-3 and CD8 expression with regard to prognosis. In contrast, in squamous cell carcinomas, better overall survival was noted primarily in cases with high stromal CD8 but not with high intraepithelial CD8. Our findings were consistent with previous studies on the prognostic impact of intraepithelial and stromal CD8$^+$ T-cells in non-small-cell lung carcinomas[37–39] and reported the differences between adenocarcinomas and squamous cell carcinomas.[40]

Both primary and secondary resistance can contribute to disease progression following treatment with anti-PD-L1/PD-1-based immunotherapy. Primary resistance, in which treatment-naïve patients show no response to initial therapy,[41] may be due to lack of tumor recognition by T cells, preexisting expression of inhibitory immune checkpoints, or other tumor-intrinsic features such as *EGFR* mutations, *ALK* translocations, *STK11* and/or *KEAP1* alterations in the setting of non-small-cell lung carcinomas.[42] In secondary resistance, an initial treatment response is thwarted by

adaptive changes, such as impaired antigen processing and presenting machinery including downregulation of HLA class-1 molecules and β_2 microglobulin, neoantigen depletion, loss of IFN-γ sensitivity, upregulation of inhibitory immune checkpoints, and release of cytokines such as TNFα to the tumor microenvironment.[43] Depending on its expression level and kinetics in tumor-associated lymphocytes, LAG-3, an inhibitory immune checkpoint, may be involved in both primary and secondary resistance to immunotherapy. This study focused on the baseline LAG-3 expression in lung adenocarcinomas and squamous cell carcinomas and explored its potential role in primary resistance in pembrolizumab-treated patients.

The reported discrepancies regarding the role of LAG-3 in non-small-cell lung carcinomas in several prior studies may be attributed to differences in the cohort composition, differences in the cutoffs used to stratify LAG-3 expression,[20–23] and the confounding effects due to the association of LAG-3 with CD8 and PD-L1. While positive correlation of LAG-3 with CD8 abundance[21–23] and tumor PD-L1 expression[21,22] were identified across several studies including herein, there were conflicting reports on the association of LAG-3 with histotypes. Although no associations of LAG-3 with histotypes were noted in two studies,[20,21] we found higher LAG-3 expression in squamous cell carcinomas as compared with adenocarcinomas, consistent with He et al.,[22] as well as higher LAG-3 expression in solid-predominant adenocarcinomas as compared with adenocarcinomas with other predominant patterns. While no associations of LAG-3 with *EGFR* status were noted in two prior studies,[20,22] we found lower LAG-3 expression in *EGFR*-mutated adenocarcinomas, which is expected given their lower immunogenicity, tumor mutational burden,[44] and PD-L1 expression[26] as compared with *EGFR* wild-type counterparts.

Likewise, the relationship between LAG-3 expression and survival appears complex. Across multiple studies and among different cohorts within the same study, high LAG-3 has been reported to be associated with worse survival, better survival, or no effect.[20–22] Of note, Hald et al. found that high LAG-3 was associated with improved survival in squamous cell carcinomas but not in adenocarcinomas.[21] In this study, we found that high LAG-3 expression was associated with worse overall survival in the entire resected non-small-cell lung carcinoma cohort, the effects were driven primarily by adenocarcinomas, and LAG-3 expression was not associated with survival in squamous-cell carcinomas. We also found that high CD8 expression was associated with better overall and recurrence-free survival in resected squamous cell carcinomas, consistent with the known association between CD8 abundance and improved outcomes in solid tumors.[45] Furthermore, this histotype-dependent association of LAG-3 with survival was noted, regardless of the medians used to stratify LAG-3 expression. Given that LAG-3 expression is mechanistically linked with diverse markers of activation, proliferation, and cytotoxic/effector functions in the tumor microenvironment,[20] additional studies are needed to reconcile these discrepancies in the prior literature and to refine our understanding on the immunomodulatory environments in non-small-cell lung carcinomas of different histologies.

The limited efficacy of immune checkpoint blockade in advanced non-small-cell lung carcinomas emphasizes the need to identify additional biomarkers to predict treatment response. In our exploratory analysis on LAG-3 in patients treated with pembrolizumab, patients were selected for treatment on the basis of high PD-L1 expression (tumor proportion score ≥50%). Compared with the entire resected tumor cohort, the higher number of LAG-3$^+$ tumor-associated lymphocytes in the pretreatment samples of the pembrolizumab-treated cohort is likely due to several factors, including higher PD-L1 expression and more advanced clinical stages, each of which is associated with high LAG-3 expression. Our findings of the association between high LAG-3 expression and improved progression-free survival appeared to contrast with Datar et al. that reported reduced progression-free survival in advanced lung cancer patients with high LAG-3.[20] Nonetheless, there were several differences between these studies: this study included only patients treated by first-line pembrolizumab, evaluated LAG-3 by immunohistochemistry, and utilized the median as the cutoff for high expression. On the other hand, Datar et al. included patients treated by various lines of PD-1 axis blockade, evaluated LAG-3 using multiplex immunofluorescence, and utilized the top 15th percentile of the entire cohort as the cutoff for high expression.[20] Furthermore, in contrast to the predictive significance of CD8 with both progression-free and overall survival, no predictive significance of LAG-3/CD8 index with survival was noted (Fig. 4), raising a possibility that high LAG-3 simply reflects high CD8 and the general inflammatory milieu, particularly given that LAG-3 correlates positively with CD8 (Supplemental Fig. 2A). Definitive assessment on the predictive significance of LAG-3 will thus require reappraisal in larger immunotherapy-treated patient cohorts with standardized inclusion criteria, methods, and cutoff values.

This study has several limitations. First, in the resected tumor cohort, while we could detect significant correlations with overall survival (such as high LAG-3 and advanced clinical stage with worse overall survival in adenocarcinomas; Fig. 3H, J), these associations were not identified with regard to recurrence-free survival (Supplemental Fig. 6H, J), suggesting that this study might not be optimally powered in assessing their associations with recurrence-free survival. Second, our assessment on the resected tumor cohort relies on the use of tissue microarrays and may be limited by intratumoral heterogeneity. Nevertheless, we attempted to reduce this variability by systematically analyzing two cores per tumor (one each from the tumor center and the invasive front), by analyzing a large number of tumors with different histologic patterns, and by analyzing separately the stromal and intraepithelial components of LAG-3 and CD8.[38,39,46–51] Our current methodology is in keeping with the clinically relevant scenarios of small biopsy-based diagnosis and biomarker classification. Third, we used the LAG-3/CD8 index as a surrogate for LAG-3 expression in lymphocytes to control for CD8$^+$ T-cell abundance, but this does not account for LAG-3 expression by other immune cells such as regulatory and natural-killer T cells.[52] Although alternate methods such as multiplex immunofluorescence can precisely measure LAG-3 expression in defined immune cell types, we opted for single chromogenic immunohistochemistry due to considerations for clinical applicability.

In conclusion, the clinicopathologic correlations and prognostic impact of LAG-3 in non-small-cell lung carcinoma are dependent on histotypes, suggesting differences in the immune microenvironment between lung adenocarcinomas and squamous-cell carcinomas. The predictive impact of LAG-3 remains to be determined and warrants further investigations on how LAG-3 alters the response to immunotherapy treatment, in the context of the complex immune microenvironments in non-small-cell lung carcinomas.

DATA AVAILABILITY

The datasets used and/or analyzed during the current study are available from the corresponding author on reasonable request.

REFERENCES

1. Vokes, E. E. et al. Nivolumab versus docetaxel in previously treated advanced non-small cell lung cancer (CheckMate 017 and CheckMate 057): 3-year update and outcomes in patients with liver metastases. *Ann. Oncol.* **29**, 959–965 (2018).
2. Paz-Ares, L. et al. Pembrolizumab plus chemotherapy for squamous non–small-cell lung cancer. *N. Engl. J. Med.* **379**, 2040–2051 (2018).

3. Reck, M. et al. Pembrolizumab versus chemotherapy for PD-L1–positive non–small-cell lung cancer. *N. Engl. J. Med.* **375**, 1823–1833 (2016).
4. Mok, T. S. K. et al. Pembrolizumab versus chemotherapy for previously untreated, PD-L1-expressing, locally advanced or metastatic non-small-cell lung cancer (KEYNOTE-042): a randomised, open-label, controlled, phase 3 trial. *Lancet* **393**, 1819–1830 (2019).
5. Topalian, S. L. et al. Safety, activity, and immune correlates of anti–PD-1 antibody in cancer. *N. Engl. J. Med.* **366**, 2443–2454 (2012).
6. Lantuejoul, S. et al. PD-L1 testing for lung cancer in 2019: perspective from the IASLC pathology committee. *J. Thorac. Oncol.* **15**, 499–519 (2019).
7. Fares, C. M., Allen, E. M. V., Drake, C. G., Allison, J. P. & Hu-Lieskovan, S. Mechanisms of resistance to immune checkpoint blockade: why does checkpoint inhibitor immunotherapy not work for all patients? *Am. Soc. Clin. Oncol. Educ. Book* **39**, 147–164 (2019).
8. Ruffo, E., Wu, R. C., Bruno, T. C., Workman, C. J. & Vignali, D. A. A. Lymphocyte-activation gene 3 (LAG3): the next immune checkpoint receptor. *Semin. Immunol.* **42**, 101305 (2019).
9. Triebel, F. et al. LAG-3, a novel lymphocyte activation gene closely related to CD4. *J. Exp. Med.* **171**, 1393–1405 (1990).
10. Baixeras, E. et al. Characterization of the lymphocyte activation gene 3-encoded protein. A new ligand for human leukocyte antigen class II antigens. *J. Exp. Med.* **176**, 327–337 (1992).
11. Wang, J. et al. Fibrinogen-like protein 1 is a major immune inhibitory ligand of LAG-3. *Cell* **176**, 334–347 (2018).
12. Kouo, T. et al. Galectin-3 shapes antitumor immune responses by suppressing CD8+ T cells via LAG-3 and inhibiting expansion of plasmacytoid dendritic cells. *Cancer Immunol. Res.* **3**, 412–423 (2015).
13. Andrews, L. P., Marciscano, A. E., Drake, C. G. & Vignali, D. A. A. LAG3 (CD223) as a cancer immunotherapy target. *Immunol. Rev.* **276**, 80–96 (2017).
14. Taube, J. M. et al. Differential expression of immune-regulatory genes associated with PD-L1 display in melanoma: implications for PD-1 pathway blockade. *Clin. Cancer. Res.* **21**, 3969–3976 (2015).
15. Li, F.-J., Zhang, Y., Jin, G.-X., Yao, L. & Wu, D.-Q. Expression of LAG-3 is coincident with the impaired effector function of HBV-specific CD8+ T cell in HCC patients. *Immunol. Lett.* **150**, 116–122 (2013).
16. Matsuzaki, J. et al. Tumor-infiltrating NY-ESO-1–specific CD8+ T cells are negatively regulated by LAG-3 and PD-1 in human ovarian cancer. *Proc. Natl. Acad. Sci. USA* **107**, 7875–7880 (2010).
17. Woo, S.-R. et al. Immune inhibitory molecules LAG-3 and PD-1 synergistically regulate T-cell function to promote tumoral immune escape. *Cancer Res.* **72**, 917–927 (2012).
18. Gros, A. et al. PD-1 identifies the patient-specific CD8+ tumor-reactive repertoire infiltrating human tumors. *J. Clin. Invest.* **124**, 2246–2259 (2014).
19. Demeure, C. E., Wolfers, J., Martin-Garcia, N., Gaulard, P. & Triebel, F. T. Lymphocytes infiltrating various tumour types express the MHC class II ligand lymphocyte activation gene-3 (LAG-3): role of LAG-3/MHC class II interactions in cell–cell contacts. *Eur. J. Cancer* **37**, 1709–1718 (2001).
20. Datar, I. et al. Expression analysis and significance of PD-1, LAG-3, and TIM-3 in human non–small cell lung cancer using spatially resolved and multiparametric single-cell analysis. *Clin. Cancer Res.* **25**, 4663–4673 (2019).
21. Hald, S. M. et al. LAG-3 in non-small cell lung cancer: expression in primary tumors and metastatic lymph nodes is associated with improved survival. *Clin. Lung Cancer* **19**, 249–259 (2017).
22. He, Y. et al. LAG-3 protein expression in non–small cell lung cancer and its relationship with PD-1/PD-L1 and tumor-infiltrating lymphocytes. *J. Thorac. Oncol.* **12**, 814–823 (2017).
23. Thommen, D. S. et al. Progression of lung cancer is associated with increased dysfunction of T cells defined by coexpression of multiple inhibitory receptors. *Cancer Immunol. Res.* **3**, 1344–1355 (2015).
24. Maruhashi, T., Sugiura, D., Okazaki, I. & Okazaki, T. LAG-3: from molecular functions to clinical applications. *J. Immunother. Cancer* **8**, e001014 (2020).
25. Herbst, R. S. et al. Pembrolizumab versus docetaxel for previously treated, PD-L1-positive, advanced non-small-cell lung cancer (KEYNOTE-010): a randomised controlled trial. *Lancet* **387**, 1540–1550 (2016).
26. Gainor, J. F. et al. EGFR mutations and ALK rearrangements are associated with low response rates to PD-1 pathway blockade in non–small cell lung cancer: a retrospective analysis. *Clin. Cancer Res.* **22**, 4585–4593 (2016).
27. Zhang, M. L. et al. Differential expression of PD-L1 and IDO1 in association with the immune microenvironment in resected lung adenocarcinomas. *Mod. Pathol.* **32**, 511–523 (2019).
28. Travis, W. D. et al. International Association for the Study of Lung Cancer/American Thoracic Society/European Respiratory Society international multidisciplinary classification of lung adenocarcinoma. *J Thorac. Oncol.* **6**, 244–285 (2011).
29. Moreira, A. L. et al. A grading system for invasive pulmonary adenocarcinoma: a proposal from the International Association for the Study of Lung Cancer Pathology Committee. *J. Thorac. Oncol.* **15**, 1599–1610 (2020).
30. Goldstraw, P. et al. The IASLC Lung Cancer Staging Project: proposals for revision of the TNM stage groupings in the forthcoming (eighth) edition of the TNM classification for lung cancer. *J. Thorac. Oncol.* **11**, 39–51 (2016).
31. Dias-Santagata, D. et al. Rapid targeted mutational analysis of human tumours: a clinical platform to guide personalized cancer medicine. *EMBO. Mol. Med.* **2**, 146–158 (2010).
32. Huynh, T. G. et al. Programmed Cell Death Ligand 1 expression in resected lung adenocarcinomas: association with immune microenvironment. *J. Thorac. Oncol.* **11**, 1869–1878 (2016).
33. Schindelin, J. et al. Fiji: an open-source platform for biological-image analysis. *Nat. Methods* **9**, 676–682 (2012).
34. Rosenbaum, M. W., Bledsoe, J. R., Morales-Oyarvide, V., Huynh, T. G. & Mino-Kenudson, M. PD-L1 expression in colorectal cancer is associated with microsatellite instability, BRAF mutation, medullary morphology and cytotoxic tumor-infiltrating lymphocytes. *Mod. Pathol.* **29**, 1104–1112 (2016).
35. Team RC. R: a language and environment for statistical computing (R Foundation for Statistical Computing, 2020) [Internet]. https://www.R-project.org/.
36. Parra, E. R. et al. Image analysis–based assessment of PD-L1 and tumor-associated immune cells density supports distinct intratumoral microenvironment groups in non–small cell lung carcinoma patients. *Clin. Cancer Res.* **22**, 6278–6289 (2016).
37. Paulsen, E.-E. et al. Assessing PDL-1 and PD-1 in non–small cell lung cancer: a novel immunoscore approach. *Clin. Lung Cancer* **18**, 220–233 (2017).
38. Al-Shibli, K. I. et al. Prognostic effect of epithelial and stromal lymphocyte infiltration in non–small cell lung cancer. *Clin. Cancer Res.* **14**, 5220–5227 (2008).
39. Donnem, T. et al. Stromal CD8+ T-cell density—a promising supplement to TNM staging in non–small cell lung cancer. *Clin. Cancer Res.* **21**, 2635–2643 (2015).
40. Andersen, S. et al. Diverging prognostic impacts of hypoxic markers according to NSCLC histology. *Lung Cancer* **72**, 294–302 (2011).
41. Sharma, P., Hu-Lieskovan, S., Wargo, J. A. & Ribas, A. Primary, adaptive, and acquired resistance to cancer immunotherapy. *Cell* **168**, 707–723 (2017).
42. Boyero, L. et al. Primary and acquired resistance to immunotherapy in lung cancer: unveiling the mechanisms underlying of immune checkpoint blockade therapy. *Cancers* **12**, 3729 (2020).
43. Ribas, A. Adaptive immune resistance: how cancer protects from immune attack. *Cancer Disco.* **5**, 915–919 (2015).
44. Willis, C. et al. Tumor mutational burden in lung cancer: a systematic literature review. *Oncotarget* **10**, 6604–6622 (2019).
45. Gentles, A. J. et al. The prognostic landscape of genes and infiltrating immune cells across human cancers. *Nat. Med.* **21**, 938–945 (2015).
46. Hendry, S. et al. Assessing tumor-infiltrating lymphocytes in solid tumors. *Adv. Anat. Pathol.* **24**, 311–335 (2017).
47. Bremnes, R. M. et al. The role of tumor-infiltrating lymphocytes in development, progression, and prognosis of non–small cell lung cancer. *J. Thorac. Oncol.* **11**, 789–800 (2016).
48. Geng, Y. et al. Prognostic role of tumor-infiltrating lymphocytes in lung cancer: a meta-analysis. *Cell Physiol. Biochem.* **37**, 1560–1571 (2015).
49. Brambilla, E. et al. Prognostic effect of tumor lymphocytic infiltration in resectable non–small-cell lung cancer. *J. Clin. Oncol.* **34**, 1223–1230 (2016).
50. Mignon, S. et al. The relationship between tumor-infiltrating lymphocytes, PD-L1 expression, driver mutations and clinical outcome parameters in non-small cell lung cancer adenocarcinoma in patients with a limited to no smoking history. *Pathol. Oncol. Res.* **26**, 1221–1228 (2020).
51. Schalper, K. A. et al. Objective measurement and clinical significance of TILS in non–small cell lung cancer. *J. Natl Cancer Inst.* **107**, dju435 (2015).
52. Anderson, A. C., Joller, N. & Kuchroo, V. K. Lag-3, Tim-3, and TIGIT: co-inhibitory receptors with specialized functions in immune regulation. *Immunity* **44**, 989–1004 (2016).

ACKNOWLEDGEMENTS

We thank Mayerling R. Dada and Alexis J. Aviles at the Massachusetts General Hospital for administrative and digital pathology support.

AUTHOR CONTRIBUTIONS

D.J.S., Y.P.H., and M.M.-K. designed the study. D.J.S., E.S.T., M.L.Z., M.K., J.B., D.A.Q., M.J. M., J.F.G., Y.P.H., and M.M.-K. performed data acquisition. D.J.S., K.K., Y.P.H., and M.M.-K. performed statistical analysis and data interpretation. D.J.S., Y.P.H., and M.M.-K. wrote the paper. All authors read and approved the paper.

FUNDING

M.M.-K. was partially supported by funding from R01 CA240317.

COMPETING INTERESTS

M.J.M. serves as a consultant and/or has received honorarium from AstraZeneca Pharmaceuticals, Nektar Therapeutics, Catalyst Pharmaceuticals, and Immunia. J.F.G. has served as a compensated consultant or received honoraria from Bristol-Myers Squibb, Genentech, Ariad/Takeda, Loxo/Lilly, Blueprint, Oncorus, Regeneron, Gilead, AstraZeneca, Pfizer, Incyte, Novartis, Merck, Agios, Amgen, and Array; research support from Novartis, Genentech/Roche, and Ariad/Takeda; institutional research support from Bristol-Myers Squibb, Tesaro, Moderna, Blueprint, Jounce, Array Biopharma, Merck, Adaptimmune, Novartis, and Alexo; and has an immediate family member who is an employee with equity at Ironwood Pharmaceuticals. M.M.-K. has served as a compensated consultant for H3 Biomedicine and AstraZeneca, has received institutional research grant support from Novartis, and has received royalty from Elsevier, all unrelated to the current study. Y.P.H. has received royalty from Elsevier unrelated to the current study. The remaining authors have no disclosures.

ETHICS APPROVAL/CONSENT TO PARTICIPATE

This study was approved by the Massachusetts General Hospital Institutional Review Board in Boston, MA, USA.

ADDITIONAL INFORMATION

Supplementary information The online version contains supplementary material available at https://doi.org/10.1038/s41379-021-00974-9.

Correspondence and requests for materials should be addressed to Mari Mino-Kenudson.

Reprints and permission information is available at http://www.nature.com/reprints

Publisher's note Springer Nature remains neutral with regard to jurisdictional claims in published maps and institutional affiliations.